

STRESS TRANSFER EFFICIENCY IN CARBON NANOTUBE BASED ROPES

Luis Zalamea* and R. Byron Pipes** [R. Byron Pipes]: bpipes@purdue.edu

**Schools of Materials Engineering, Aeronautics and Astronautics,

*Chemical Engineering and Birck Nanotechnology Center,
Purdue University, West Lafayette, IN 47907-2044, USA

Keywords: *Carbon Nanotubes, Helical Ropes, Shear Lag, Stress Transfer*

1 Introduction

Semi-empirical models derived for pseudo homogeneous ropes [1] have been employed to calculate the effective stiffness of ropes made out of MWNT [2]. Those approximate models predict a significant reduction with respect to the Young's modulus of an individual filament by considering the effect of miss-orientation of the twisted filament with respect to the applied load, migration of filaments within the fiber and radial compression. Such models do not explicitly take into account the load transfer efficiency from the rope to an individual fiber, but have provided satisfactory approximate results, and a convenient way to understand and compare experimental data reported recently on macroscopic array.

Several variations of the standard shear lag model can be employed as an alternative to estimate load transfer from a matrix into a fiber of finite length embedded in a homogeneous media composed by the other fibers [3].

The main objective of the present work is to employ previously calculated values of shear stiffness of single walled carbon nanotube arrays [4] to estimate the magnitude of overlap length necessary to attain efficient load transfer between filaments in a rope. On a first approximation the model neglects the effects of helical wrapping which has been demonstrated to be of second order for ropes less than approx. 40nm dia.. This poses a problem because it invalidates one possible mechanism for enhancement of load transfer; the radial stress generated due to frictional forces. The results obtained indicate that due to the low interfacial shear modulus, the lengths necessary to attain a significant fraction of the stiffness of the constituent filament are on the order of several microns. Fabrication techniques capable of conferring such degree of perfection at that scale, in a rope do not exist at the present time.

2 Model Development

2.1 Geometry Conversion

The effective modulus of an individual carbon nanotube under tension or flexure is not equivalent to that of a graphene sheet, since there is an area at the center that must be taken into account and does not contribute to the stiffening of the structure.

The assumed wall thickness is equivalent to the separation distance between two consecutive graphene layers, which can vary from 0.31 to 0.39 according to experimental reports [5]. This framework insures that no structure based on folded and rolled graphene sheets can have stiffness larger than that of graphite.

For SWNT the assumed wall thickness is equivalent to the separation distance between two SWNT forming an array. Due to this approximation, in the converted geometry the individual carbon nanotubes are in contact with their neighbors.

2.2 Shear Lag Models

As explained in detail elsewhere [4], in order to keep solutions for beam bending analytical, the hexagonal symmetry of the carbon nanotube array can be replaced by a rectangular equivalent, or it can be replaced by a concentric cylinder array to consider one nanotube immersed in a homogeneous matrix, as depicted in Fig. 1.

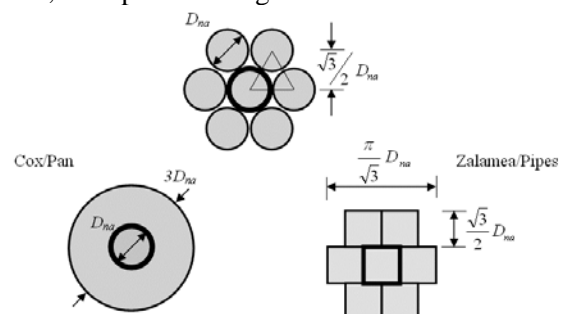


Fig. 1. Approximate Geometries for SWNT Array

A shear lag model developed to study stress transfer in concentric shells as those in MWNT [6], can be readily extended to the situation mentioned above. The input parameters are the shear stiffness of the interfacial regions and the approximations for the diameters of each layer, both of which have been calculated and reported elsewhere [4].

Typical values for the shear stiffness of the interfacial region of SWNT are as follows:

	7-Elem.	61-Elem.	127-Elem.
Interfacial Area, [m ² *10 ⁻¹⁵]	1.46	29.3	66.0
Interfacial Energy, [J/m ² *10 ⁻³]	13.1	22.1	17.5
Interfacial Modulus, [MPa]	371	236	151

Table 1. Effective Properties of the Interfacial Regions in Shear

The bold segment of the interfacial region indicates the area over which shear stress transfer takes place, for the hypothetical situation in which the center filament is pulled by the array. Note however that the present work neglects the capillary energy component that will arise as a result of creation of new surface area. Instead, the center filament is considered to be immersed in a matrix composed of the other tubes. This assumption allows a very simple form of the shear transfer parameter β , as defined by Cox [3] in his seminal 1952 paper

The well-known analytical solution of a shear lag model with this parameter results in the following expression for the effective Young's modulus [3]:

$$\frac{E_{eff}}{E} = 1 - \frac{\tanh\left(\beta \frac{L}{2}\right)}{\beta \frac{L}{2}} \quad (1)$$

The previous equation provides a first order approximation at the efficiency to transfer load applied only to the external layer of a seven element rope into the centermost element.

The calculation of the shear transfer parameter β , has received considerable attention in the literature, especially for applications to fiber pullout tests, where the outer diameter of the structure is not clearly defined [7]. For the problem at hand it has been assumed that the external radius of the matrix is equivalent to the distance from the center of the rope to the center of the outermost layer of elements, following the work of pan [8]. This approximation

results in the following expression for the shear lag parameter:

$$\beta = \frac{1}{r_{na}} \sqrt{\frac{2}{\ln 2}} \sqrt{\frac{G_{int}}{E}} \quad (2)$$

Alternatively a shear lag analysis based on cylindrical solid bodies in contact yields the following expression for the same parameter [6]:

$$\beta = \sqrt{\left(\frac{1}{A_1} + \frac{1}{A_2}\right)} \sqrt{\frac{2\pi R_1}{h_1}} \sqrt{\frac{G_{int}}{E}} \quad (3)$$

In the previous expression, h_1 is the distance between the average radii of both cylinders, and R_1 is the average radius of the interfacial region. The shear modulus was converted from rectangular to circular geometry in Fig. 1, by considering the differences in cross sectional areas and the perimeter over which the load transfer takes place.

These variations of the shear lag parameter lead to differences in the actual value but not on the trend, as shown:

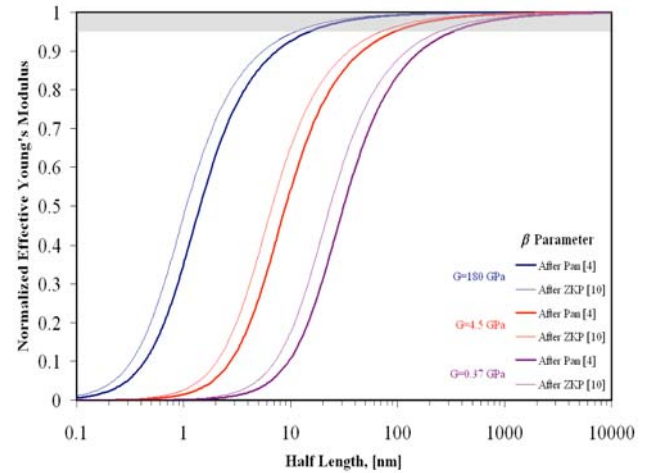


Fig. 2. Effective Young's modulus as a function of Length and Shear Stiffness ay

The differences between the two estimations of the shear lag parameter are not relevant compared to those due to the shear modulus of the interfacial region (or pseudo homogeneous matrix). A first order estimate for the stiffness of the interfacial regions in an array of carbon nanotubes, can be obtained from the corresponding value for graphite: 4.5 GPa [5], however, recent reports have employed hybrid atomistic continuum models to estimate the bounds for such elastic constant [9], and the results suggest slightly lower values, in accordance with the calculations based on energetics under flexure [4]. In principle the shear modulus of the interfacial region

can be close to that of in plane graphite (180 GPa), although it would require a very high density of crosslinks. In this case the length necessary to obtain the same efficiency is reduced drastically, as presented graphically in Fig. 2.

The main conclusion that can be drawn from Figure 4 is that there is an enormous incentive for efforts aimed at strengthening the interface, because they have very relevant effects on the overlap length necessary to insure proper load transfer. Several experimental [10,11] as well as theoretical [12,13] works have reported on this issue.

2.3 Conventional Semi-Empirical Rope Models

The book by Hearle et al.[1] was followed for the calculation of the effective Young's modulus of a helical rope (yarn). Although some parameters are empirical it can provide a first order approximation to be compared against the corresponding value from shear lag analyses presented before and experimental data [2].

There are three factors modifying the effective stiffness of a helical rope of any material: the mis-orientation of the fibers with respect to the yarn due to twisting, the radial compression due as a result of axial deformation (Poisson's effect) of the yarn as well as the fibers, and finally the finite length of constituent fibers, which results in the necessity of migration as a mechanism to insure cohesion in the rope, as hypothesized by Hearle et al. in their book.

The following equation combines the effects of mis-orientation, radial contraction and finite length:

$$\frac{E_{eff}}{\phi E} = \cos^2 \alpha (1 - k \csc \alpha) F_v \quad (4)$$

$$k = \frac{\sqrt{2}}{3L_f} \sqrt{\frac{D_f Q}{\mu}}$$

The factor α is the helical angle to which the individual fibers are twisted in order to form a cohesive yarn.

The Poisson's or radial contraction effect can be calculated by means of the following equation:

$$F_v = \frac{2}{(1+2\nu_f)\sin^2 \alpha} \left[\frac{(1+\nu_y) \left(\ln(\cos \alpha) + \frac{2(1+\nu_f)}{1+2\nu_f} (1 - \cos \alpha^{2\nu_f+1}) \right)}{2 \left(\frac{\nu_y}{2\nu_f-1} (3(1+2\nu_f) - \frac{4(1+\nu_f)}{2\nu_f-1} \cos \alpha^{2\nu_f-1} - \frac{1}{\cos^2 \alpha}) \right)} \right] \quad (5)$$

This effect might be especially important, as indicated by the experimental findings of Baughman

and coworkers, who observed unusually large Poisson's ratios for yarns made out of multiwalled carbon nanotubes. However such large contractions must be analyzed carefully to understand their relationship with changes in packing and volume fraction

Finally the effect of finite length of the fibers was treated by Hearle et al. assuming that all fibers slowly migrate radially across the yarn, providing a mechanism to accommodate finite length fibers without losing cohesion.

In equation (5) μ is the friction coefficient between fibers ($F=\mu N$) and Q is the migration length, i.e., the length necessary for a fiber to migrate all the way from the outer surface to the center and back to the surface of the yarn. D_f is the diameter of a fiber and L_f is its length.

The migration length should be smaller than the fiber length in order for the stress transfer mechanism to be fully effective. However it would be possible to have migration lengths larger than the fiber length and still have some degree of load transfer. In the limit, the migration length becomes infinite and the stiffness reduces to zero.

The values used for the calculation of effective modulus as a function of fiber length are presented in Table 2, and the results are plotted in Figs. 5-6.

Parameter	Value
Helical Angle	25 deg
Yarn diameter	2 μm
Fiber diameter	10 nm
Fiber Length	100 μm
Yarn Poisson's R.	2.0-2.7 ²
MWNT Poisson's R.	0.1-0.3 ¹⁴
Migration Length	10-1000 μm
Friction Coefficient	0.1-0.3 (?)

Table 2. Yarn and Fiber Properties for Hearle's Models

The values of shear modulus estimated from flexural experiments cannot be used directly to estimate a friction coefficient because there is no unique relationship between both. The radial compression effect was calculated for a yarn Poisson's ratio of 2.35 and a fiber Poisson's ratio of 0.2. The shaded region indicates the range of lengths measured by Baughman and coworkers in their report.

The following figure was generated using a value of 0.2 for the friction coefficient. Recent experiments of graphite [15] suggest that it could eventually deviate appreciably from the assumed value if the two graphene surfaces are not

commensurate with each other. It could be negligibly small resulting in a very large impact on the stiffness, as presented graphically on Fig. 4, in which the migration length was kept constant at 0.1 mm (100µm, equivalent to the fiber length).

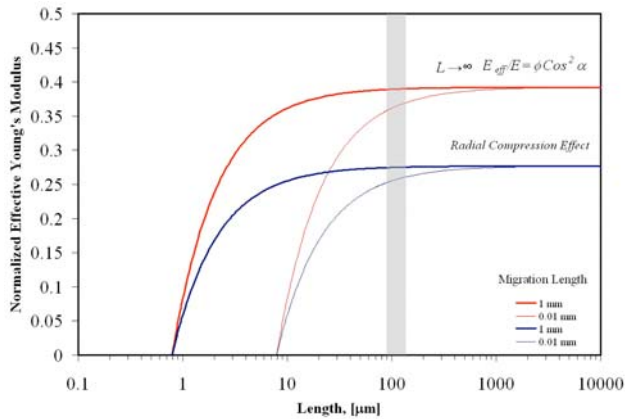


Fig. 4. Modeling Baughman's Experiments

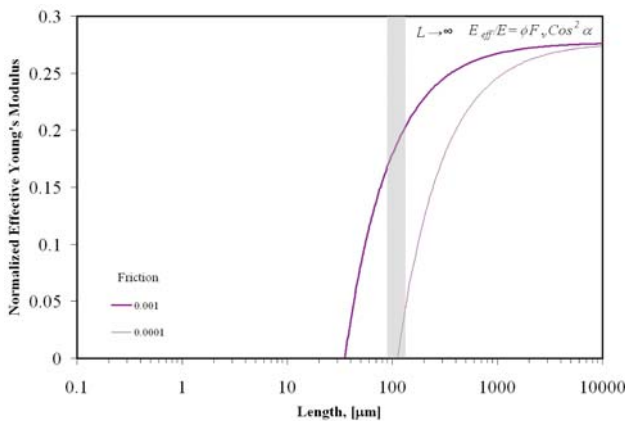


Fig. 5. Ultralow Friction Coefficient

Interestingly, for the lengths reported by Baughman et al. [2] and usual macroscopic values of the friction coefficient (~0.1), Hearle's models predict a rather mild decrease in stiffness, unless the migration length falls below its critical limit. In contrast, their experiments show a drastic reduction in stiffness. i.e., the effective modulus measured is only 1.23% of the expected value, taking into account reductions by volume fraction, hexagonal packing fraction and the fact that the constituent nanotubes are partially hollow. The explanation for this unusually low value may lie in the surprisingly low value of the friction coefficient for graphitic structures.

2.4 Model Comparison

The following plot presents a comparison between the two models, showing that very low

friction coefficients or shear modulus are responsible for the low effective stiffness:

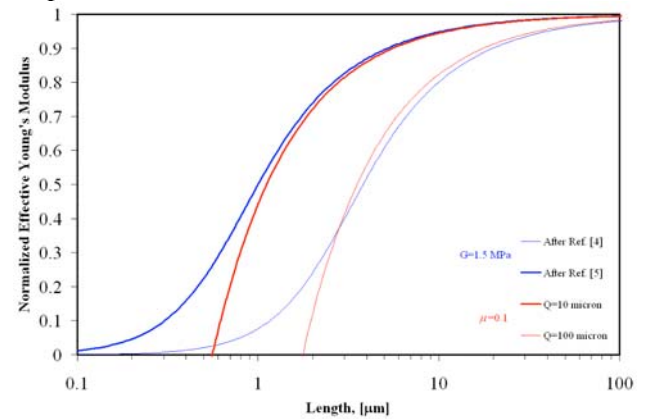


Fig. 6. Model Comparisons

The value of the interfacial shear modulus that corresponds to a friction coefficient of ~0.1 is very low and close to the corresponding value reported for graphite [15]. For very low friction coefficients as those mentioned above, the corresponding shear stiffness becomes negligibly small.

2.5 Conclusions

According to the experimental data analyzed, the overlap necessary to insure proper load transfer among untwisted SWNT is rather large (on the order of microns). Fabrication techniques aimed at optimizing the overlap length would enhance significantly the load transfer efficiency of ropes. Interestingly, very short overlap lengths would be enough to transfer load satisfactorily, provided they are chemically modified to increase the interfacial shear stiffness. There are great, yet unexploited, potential benefits for surface modified carbon nanotube systems (both SWNT and MWNT) that have not been realized on a macroscopic scale.

In the case of MWNT, the capillary forces are not as effective because the strength of the interaction decreases as size increases, as calculated by Girifalco et al. [16]. However experimental evidence suggests that friction between shells in MWNT can be very low facilitating sliding of one MWNT past another and making large overlap lengths theoretically possible. Frictional resistance among MWNT is still a subject of debate and it is a very relevant parameter in the design of ropes, as demonstrated by the calculations presented

To summarize, the design of CNT structures should be addressed on a multiscale manner, seeking to extract advantages of the different load transfer mechanisms that dominate each scale. i.e. commensurability and shear stiffness at the

nanoscale, and twisting-induced stresses at the microscale

References

- [1] J.Hearle, et al., *Structural Mechanics of Fibers, Yarns and Fabrics*, V.1, Wiley-Interscience, (1969).
- [2] M.Zhang, et al., Multifunctional Carbon Nanotube Yarns, *Science*, **306**(5700), 1358 (2004).
- [3] H.Cox, Elasticity and Strength of Paper and Other Fibrous Materials, *Brit. J. Appl. Phys.* **3**, 72. (1952).
- [4] R.B.Pipes, et al., Flexural Deflection as a Measure of van der Waals Interaction, *Comp.Sci&Tech.*, 66(9), 1122, (2006).
- [5] M.Dresselhaus, et al., *Carbon Nanotubes*, Springer-Verlag, (2000).
- [6] Zalamea et al., Stress Transfer in Multiwalled Carbon Nanotubes, *in press in Comp.Sci&Tech.*
- [7] J.A. Nairn, On the Use of Shear-Lag Methods for Analysis of Stress Transfer in Unidirectional Composites, *Mechanics of Materials*, **26**, 63, (1997)
- [8] N. Pan, Development of a Constitutive Theory for Short Fiber Yarns: Mechanics of Staple Yarn Without Slippage Effect, *Textile Res. J.*, **62**(12), 749, (1992)
- [9] J.Z. Liu, Q.S. Zheng, L.F. Wang, Q. Jiang, Mechanical properties of single-walled carbon nanotube bundles as bulk materials, *Journal of Mechanics and Physics of solids*, **53**, 123, (2005)
- [10] W. Guo, W. Zhong, Y. Dai, and S. Li, Coupled defect-size effects on interlayer friction in multiwalled carbon nanotubes, *Phys. Rev. B*, **72**, 075409 (2005)
- [11] M. Huhtala, A.V. Krascheninnikov, J. Aittoniemi, S.J. Stuart, K. Nordlund, and K. Kaski, Improved mechanical load transfer between shells of multiwalled carbon nanotubes, *Phys. Rev. B*, **70**, 045404 (2004)
- [12] J.P. Salvetat, et al., Elastic and Shear Moduli of Single-Walled Carbon Nanotube Ropes, *Phys. Rev. Lett.*, **82**(5), 944, (1999)
- [13] Cs. Mikó, M. Milas, J.W. Seo, R. Gaál, A. Kulik, and L. Forró, Effect of ultraviolet light irradiation on macroscopic single-walled carbon nanotube bundles, *Appl. Phys. Lett.*, **88**, 151905, (2006)
- [14] L. Shen and J. Li, Transversely isotropic elastic properties of multiwalled carbon nanotubes, *Phys. Rev. B*, **71**, 035412 (2005)
- [15] M. Dienwiebel, G.S. Verhoeven, N. Pradeep, J.W.M. Frenken, J.A. Heimberg and H.W. Zandbergen, Superlubricity of Graphite, *Phys. Rev. Lett.*, **92**, 126101, (2004)
- [16] L.A. Girifalco, M. Hodak, and R.S. Lee, Carbon nanotubes, buckyballs, ropes, and a universal graphitic potential, *Phys. Rev. B*, **62**(19), 13104, (2000)